JOURNAL OF TISSUE ENGINEERING AND REGENERATIVE MEDICINE
J Tissue Eng Regen Med 2010; **4**: 444–453.
Published online 28 January 2010 in Wiley InterScience (www.interscience.wiley.com) **DOI:** 10.1002/term.255

RESEARCH ARTICLE

Surface modification of a biodegradable composite by UV laser ablation: *in vitro* biological performance

Albino Martins[1,2]*, Wu Gang[3], Elisabete D. Pinho[1,2], Esther Rebollar[3], Stefano Chiussi[3], Rui L. Reis[1,2], Betty León[3] and Nuno M. Neves[1,2]

[1]*3B's Research Group – Biomaterials, Biodegradables and Biomimetics, Department of Polymer Engineering, University of Minho, and Headquarters of the European Institute of Excellence on Tissue Engineering and Regenerative Medicine, AvePark, Zona Industrial da Gandra, S. Cláudio do Barco, 4806-909 Caldas das Taipas, Guimarães, Portugal*
[2]*Institute for Biotechnology and Bioengineering (IBB), PT Government Associated Laboratory, Braga, Portugal*
[3]*Departamento de Física Aplicada, ETSI Industriales, Universidad de Vigo, Lagoas Marcosende s/n, 36310 Vigo, Spain*

Abstract

Melt blends of chitosan and biodegradable aliphatic polyester have been physically and biologically studied, presenting great potential for biomedical applications. Structurally, poly(butylene succinate)–chitosan (PBS/Cht) composite scaffolds are covered by a thin PBS layer, preventing the desired interaction of cells/tissues with the chitosan particules. In the present work, a selective and controlled ablation of this skin layer was induced by UV laser processing. X-ray photoelectron spectroscopy (XPS) and time-of-flight secondary ion mass spectrometry (ToF–SIMS) data demonstrated an increment of chitosan components and others resulting from the laser ablation process. The biological activity (i.e. cell viability and proliferation) on the inner regions of the composite scaffolds is not significantly different from those of the external layer, despite the observed differences in surface roughness (determined by interferometric optical profilometry) and wettability (water contact angle). However, the morphology of human osteoblastic cells was found to be considerably different in the case of laser-processed samples, since the cells tend to aggregate in multilayer columnar structures, preferring the PBS surface and avoiding the chitosan-rich areas. Thus, UV laser ablation can be considered a model technique for the physical surface modification of biomaterials without detrimental effects on cellular activity. Copyright © 2010 John Wiley & Sons, Ltd.

Received 2 November 2009; Accepted 11 November 2009

Keywords **surface modification; biodegradable composite; laser ablation; surface properties; biological performance**

1. Introduction

Biodegradable polymers have been thoroughly explored as biomaterials in the field of tissue engineering and regenerative medicine. A number of naturally-derived polymers (e.g. collagen, gelatin, fibrin, chitosan and starch; Malafaya *et al.*, 2003; Mano *et al.*, 2007) and synthetic polymers, such as polycaprolactone (PCL), poly(lactic acid) (PLA), poly(glycolic acid) (PGA), poly(ethylene) gylcol (PEG), poly(vinyl alcohol) (PVA) and polyurethane (PU) (Agrawal and Ray, 2001; Gomes and Reis, 2004; Lutolf and Hubbell, 2005) are already being employed for biomedical applications. Blends made of synthetic and natural biodegradable polymers can be designed and tailored to obtain a wide range of desirable properties in exquisite combinations (i.e. mechanical properties, degradation, hydrophilicity and biocompatibility). It is possible to combine the processing freedom offered by the synthetic polymers with the biocompatibility and excellent biological interface of natural polymers with cells (Correlo *et al.*, 2005; Sarasam and Madihally, 2005; Correlo *et al.*, 2008). Indeed, natural-origin polymers offer the advantage of being

*Correspondence to: Albino Martins, 3B's Research Group – Biomaterials, Biodegradables and Biomimetics, Department of Polymer Engineering, University of Minho, Guimarães, Portugal. E-mail: amartins@dep.uminho.pt

similar to native extracellular matrix macromolecules. Furthermore, these polymers present the attractive characteristic of being degraded by naturally occurring enzymes and, eventually, metabolized by physiological mechanisms.

Chitosan (Cht), is the alkaline deacetylated product of chitin, which is the second most abundant polysaccharide after cellulose (Rinaudo *et al*., 1993). Structurally, it has similarities with glycosaminoglycans of the native extracellular matrix found in different human tissues. Chitosan was already reported to be non-toxic, biodegradable and biocompatible (Kim *et al*., 2007; VandeVord *et al*., 2002; Cruz *et al*., 2008). A solution to improve its processability and physical properties is blending with other polymers. Different polymers, including polyvinyl alcohol (PVA) (Chuang *et al*., 1999; Koyano *et al*., 1998; Mucha and Pawlak, 2005), poly(lactic acid) (PLA) (Wan *et al*., 2006), polyethylene glycol (PEG) (Kolhe and Kannan, 2003), polycaprolactone (PCL) (Honma *et al*., 2006; Im *et al*., 2003; Sarasam and Madihally, 2005), polyethylene oxide (PEO) (Subramanian *et al*., 2005; Zivanovic *et al*., 2007), hydroxypropylcellulose (HPC) (Mucha and Pawlak, 2005), collagen (Arpornmaeklong *et al*., 2007; Ma *et al*., 2003; Wu *et al*., 2007), silk fibroin (Gobin *et al*., 2005) and hyaluronan (Chen *et al*., 2005; Liu *et al*., 2007; Majima *et al*., 2007) have been combined with chitosan to obtain materials with desirable mechanical and biological properties.

Among the many synthetic biodegradable polymers proposed, poly(butylene succinate) (PBS) has been recently shown to have interesting physical and biological properties when combined with chitosan (Correlo *et al*., 2005, 2007, 2008; Costa-Pinto *et al*., 2008; Coutinho *et al*., 2008; Oliveira *et al*., 2008; Pinho *et al*., 2008). PBS is an aliphatic thermoplastic polyester (Gan *et al*., 2001; Ray *et al*., 2002), which was developed and commercialized by Showa HighPolymer under the trade name Bionelle® and proposed for diverse applications, such as agriculture, fishery, forestry and civil engineering, and for common household goods. Previous studies showed that when the PBS/chitosan (PBS/Cht) composite is fabricated by screw extrusion moulding, injection moulding or compression moulding methods, a PBS-rich layer is formed on the surface of the composite structure, preventing the desired interactions of cells/tissues with the chitosan (Correlo *et al*., 2005, 2008; Pinho *et al*., 2008).

Since the referred polymeric composite has been proposed for biomedical applications (Costa-Pinto *et al*., 2008; Oliveira *et al*., 2008), the influence of the inner scaffold regions over cellular performance represents an important aspect to be determined. We here propose the use of UV laser ablation to selectively remove the PBS-thin layer that covers PBS/Cht composite scaffolds. Pulsed-laser ablation allows the controlled removal of a component with high spatial resolution, both laterally and in depth, without damage to the underlying substrate. Surface properties such as roughness, wettability and chemical composition, which are known to control cell response to a biomaterial, were evaluated. The influence of the materials' distribution in the composite was analysed both at the surface and in the bulk of the scaffold, based on the behaviour of human osteoblastic cells (Saos-2 cell line).

2. Materials and methods

2.1. Materials processing

The PBS/Cht composite (50 : 50 wt.%) was prepared from medium molecular weight ($M_v = 416$ kDa) chitosan (particle size 15–145 μm) with a degree of deacetylation of approximately 85%, supplied by France Chitin (Orange, France), and PBS Bionelle™ 1050 (Showa Highpolymer Co. Ltd., Tokyo, Japan). The materials (PBS/Cht or PBS) were processed into disk samples (10 mm diameter and 1 mm thick) by injection moulding (using an Engel injection moulding machine). Further details on the processing parameters of these materials can be found elsewhere (Correlo *et al*., 2005).

The samples were irradiated in an air atmosphere by an ArF excimer laser (Lambda Physik LPX220i, 193 nm, 20 ns FWHM) focused by a homogenizer (Microlas) at normal incidence onto an area of ~0.1 cm^2. Energy was measured by an energy radiant meter (Oriel 70 260). Before the laser etching of the discs, the optimal irradiation parameters for the removal of the external PBS-rich layer were determined.

2.2. Surface morphology characterization

Chitosan particules distribution in the polymer matrix was assessed by eosin staining. After ablation, the samples were immersed into a 0.10 (w/v)eosin alcohol solution for 5 min, then cleaned in distilled water in an ultrasonic bath for 3 min and washed several times with distilled water in order to remove the residual eosin. Photographs of the stained surface were obtained by an optical microscope equipped with a CCD camera and image recording software. The pictures were then processed by the software Image Pro Plus 6, which automatically calculates the chitosan area.

The surface roughness of the samples was analysed by interferometric optical profilometry. A surface profiler (DEKTAK^{3}ST, Veeco, USA) was used to measure the surface roughness and crater depth after ablation. For the surface roughness determination, the stylus was linearly scanned in soft touch mode, both inside and outside the irradiated area over a length of 500 μm. The horizontal resolution was 1 μm/sample point. The roughness average (R_a) values were automatically calculated by the equipment analytical software WycoVision® 32.

The wettability of the surfaces was assessed by contact angle measurements. Measurements of the static contact angle were carried out at room temperature, using

DOI: 10.1002/term

the sessile drop method and contact angle equipment (Model OCA 15plus, DataPhysics Instruments, Germany) coupled to a high performance image processing system. A standard polar liquid water (2 µl, HPLC grade), was dispensed using a motor-driven syringe at different zones of each sample and the measurement time extended to 10 min. At least five measurements were carried out for each sample and statistical analysis was performed.

2.3. Surface chemistry characterization

The chemical characterization of the surfaces was first performed by Attenuated Total Reflection-Fourier Transform InfraRed (ATR–FTIR). The FTIR spectra were recorded on an IRPrestige 21 FTIR spectrophotometer (Shimadzu, Japan) with a resolution of 4 cm^{-1} and averaged over 10 scans.

X-ray photoelectron spectroscopy (XPS) measurements were performed for a detailed analysis of the chemical composition of the irradiated and non-irradiated samples. The XPS analysis was performed using a VG Escalab 250 iXL ESCA instrument (VG Scientific, UK), using monochromatic Al-Kα radiation ($h\nu = 1486.92$ eV). Photoelectrons were collected from a take-off angle of 90° relative to the sample surface. The measurement was pereformed in a constant analyser energy (CAE) mode with 100 eV pass energy for survey spectra and 20 eV pass energy for high-resolution spectra. Charge referencing was carried out by setting the lower binding energy C1*s* hydrocarbon (CHx) peak at 285 eV.

ToF–SIMS measurements were also performed for further characterization of the chemical composition. The mass spectra of the samples were recorded on a ToF–SIMS IV instrument (Ion-Tof GmbH, Germany). The sample was bombarded with a pulsed bismuth ion beam. The secondary ions generated were extracted with a 10 kV voltage and their time of flight (ToF) from the sample to the detector was measured in a reflectron mass spectrometer. The typical analysis conditions for this work were 25 keV pulsed Bi^{3+} beam at 45° incidence, rastered over 250 × 250 μm^2, and an electron flood gun was used for charge compensation.

2.4. Biological assays

Human osteosarcoma-derived cells [Saos-2 cell line; European Collection of Cell Cultures (ECACC), UK] were maintained in Dulbecco's modified Eagle's medium (DMEM; Sigma-Aldrich, Germany) supplemented with 10% heat-inactivated fetal bovine serum (Biochrom, Berlin, Germany) and 1% antibiotic-antimycotic (Gibco, GB). The cells were cultured in a humidified incubator at 37 °C in a 5% CO_2 atmosphere, and the medium was routinely changed every 3–4 days.

Confluent osteoblast-like cells were harvested for seeding onto tissue culture polystyrene coverslips (TCPS), non-processed PBS/Cht and laser-processed PBS/Cht (PBS/Cht_laser) discs at a concentration of 3.3×10^4 cells/ml/disc. The osteoblastic cells seeded on the disc surfaces were maintained in 24-well cell culture plates (Costar®, Corning, NY) and cultured for 1, 4 and 7 days. To evaluate the cell morphology and distribution in the surface, the samples were fixed with 2.5% glutaraldehyde (Sigma, USA) in 1× phosphate buffer saline solution, pH 7.4 (Sigma, USA), for 1 h at 4 °C. Then they were dehydrated through a graded series of ethanols and allowed to dry overnight at room temperature. Finally, they were sputter-coated with gold (sputter coater, Model SC502, Fisons Instruments, UK) and analysed by scanning electron microscopy (SEM; model S360, Leica Cambridge, UK).

At each defined time culture period, the cell viability and proliferation was determined using the CellTiter 96® AQueous One Solution Cell Proliferation Assay (Promega, USA). This assay is based on the bioreduction of a tetrazolium compound, 3-(4,5-dimethylthiazol-2-yl)-5-(3-carboxymethoxyphenyl)-2-(4-sulphophenyl)-2*H*-tetrazolium (MTS) to a water-soluble brown formazan product. The absorbance, measured at 490 nm in a microplate reader (Synergie HT, Bio-Tek, USA), is related with the quantity of formazan product and directly proportional to the number of living cells in the constructs. Triplicates were characterized for every culture time period (1, 4 and 7 days).

Cell proliferation was quantified by the total amount of double-stranded DNA along the culture time. Quantification was performed using the Quant-iT® PicoGreen dsDNA Assay Kit (Invitrogen™, Molecular Probes™, OR, USA), according to the manufacturer's instructions. Briefly, cells in the construct were lysed by osmotic and thermal shock and the supernatant used for the DNA quantification assay. The fluorescence of the dye, PicoGreen, was measured at an excitation wavelength of 528/20 nm in a microplate reader (Synergie HT, Bio-Tek, USA), the intensity of the signal being proportional to the amount of DNA. Triplicates were made of each sample, allowing statistical analysis to be performed. The DNA concentration for each sample was calculated using a standard curve relating the quantity of DNA and fluorescence intensity.

3. Results and discussion

Important characteristics of scaffolds intended for tissue-engineering applications are their physicochemical surface properties, including wettability, chemical composition and roughness (Anselme *et al.*, 2000b; Hutmacher *et al.*, 2007; Salgado *et al.*, 2004). The surface of the biomaterial interacts directly with the biological environment during both *in vitro* experiments and *in vivo* implantation. Indeed, the surface properties were found to condition the adsorption of proteins and, consequently, mediate cell adhesion (Alves and Reis, 2005).

In the present study, surface modification of PBS/Cht scaffolds was induced by UV laser ablation of the PBS-rich

DOI: 10.1002/term

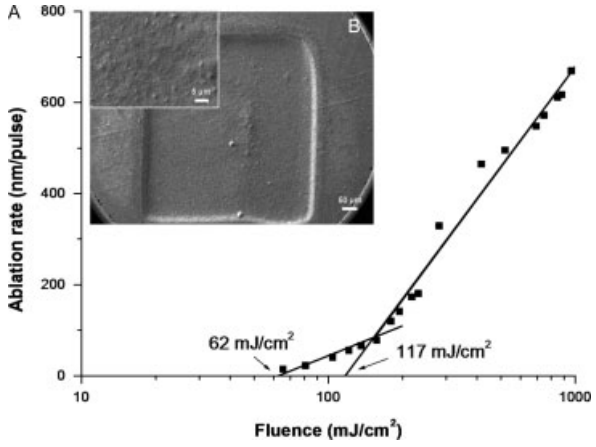

Figure 1. (A) Dependence of ablation rate on the laser fluence. (B) SEM micrographs of a laser-processed PBS/Cht disc at 150 mJ/cm^2

layer that covers the composite. To achieve that aim, the optimal irradiation parameters for its selective removal were determined. Figure 1A displays the ablation rate of the PBS/Cht composite for different laser conditions. It can be observed that data could be fitted with two different slopes. This fact could indicate two different ablation behaviours, corresponding to the skin and to the bulk of the composite scaffold. As previously reported (Correlo *et al*., 2005, 2008), the morphology of the moulded samples displays a skin–core distribution. The skin is composed almost entirely of PBS and the chitosan particles (with sizes in the range 15–145 μm) are dispersed in the PBS matrix below the skin. Because chitosan does not melt during the injection-moulding process, its viscosity is not affected by the stress and thermal history, thus causing the aggregation of the chitosan phase in the centre of the melt flow channels (Figure 1B). In opposition, PBS, which melts during injection moulding, constitutes the continuous phase of the composite. Thus, the first behaviour observed for lower-intensity laser ablation could correspond to the ablation of the external layer of PBS, while the change in the slope would indicate ablation of the underlying PBS/Cht composite. Two different ablation thresholds are identified, one for the PBS skin layer (62 mJ/cm^2) and another one for the bulk material (117 mJ/cm^2). Because the ablation threshold of PBS/Cht composite is higher than the PBS ablation threshold, by using a laser intensity between the two values we can promote the ablation of only the external PBS layer. Considering the number of pulses needed for the change of slope and, consequently, for the removal of the external layer and to reach the bulk of the disc, the thickness of this layer is estimated to be 7 ± 2 μm.

3.1. Surface morphology characterization

Figure 2A shows the dependence of roughness and chitosan content, as assessed by eosin staining, on the laser fluence. By using low fluence, below the ablation threshold, the roughness and the chitosan amount remained almost unchanged when varying the number of pulses. In this case, the fluence was not sufficient to induce ablation of the material, and the slight roughness increase corresponded to morphological changes induced in the external PBS layer. The absence of significant changes in the chitosan content confirmed that the external layer was still present and that the chitosan phase below the PBS skin remained unaffected. Conversely, higher fluence, above the higher ablation threshold of the bulk material, caused a significant ablation, demonstrated by the pronounced increase of the surface roughness and of the chitosan content. Due to the preferential ablation of PBS, the chitosan clusters appearing at the surface caused an increase of the surface roughness (Figure 2B). According to these initial experiments, the parameters for the removal of the external PBS layer were selected: laser fluence was set at 90 mJ/cm^2, above the ablation threshold of PBS and below the ablation threshold of the bulk PBS/Cht composite, the number of pulses was set at 50, and the frequency at 1 Hz.

The morphological and chemical surface changes detected after etching were further characterized by contact angle measurements. Both non-processed and laser-processed PBS/Cht samples were characterized at various time points to evaluate the evolution of the

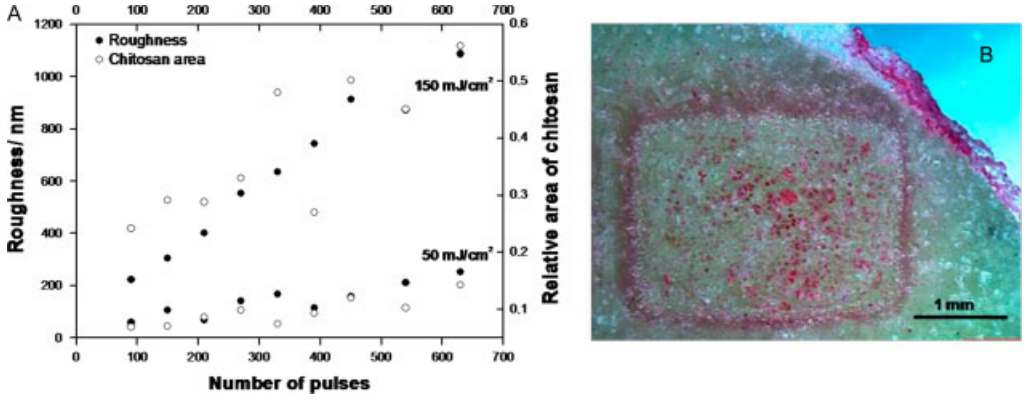

Figure 2. (A) Dependence of the surface roughness and of the relative area of chitosan on the number of pulses used for irradiation. (B) Optical microscopy image after eosin staining of a laser-processed PBS–Cht disc at 150 mJ/cm^2

DOI: 10.1002/term

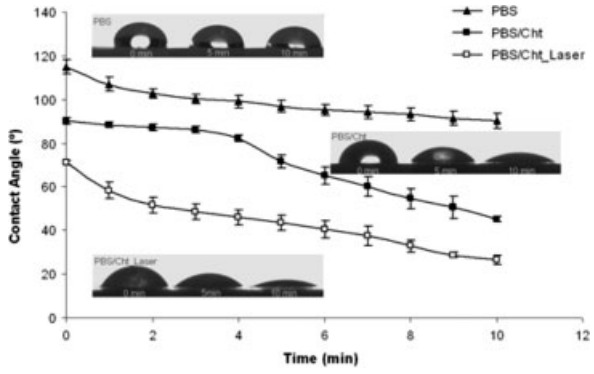

Figure 3. Water contact angle values of non-processed PBS, PBS–Cht and laser-processed PBS/Cht (PBS/Cht_Laser) discs as a function of time

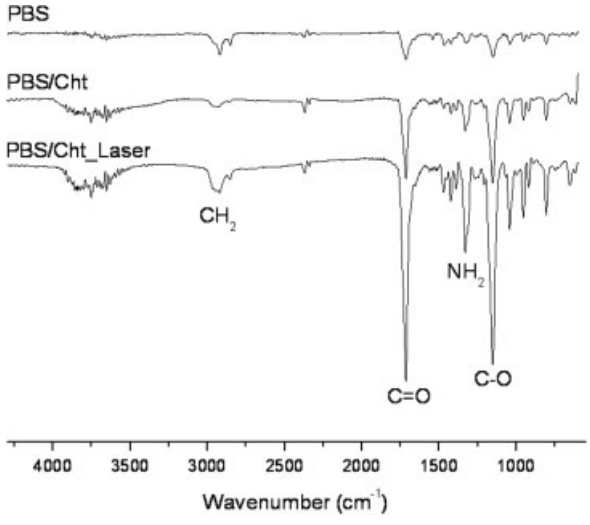

Figure 4. ATR–FTIR spectra of non-processed PBS, PBS/Cht and laser-processed PBS/Cht (PBS/Cht_laser) discs

surface properties. Non-processed PBS/Cht showed a hydrophobic character. A water contact angle of 90° was measured (Figure 3) and a sharp decrease in the contact angle was observed during the time period of the analysis (10 min). The laser processing induced a significant decrease in the water contact angle to a value of 70°, enhancing the hydrophilic character of the surfaces (Figure 3). The increment in the hydrophilicity of the surfaces after laser processing (PBS/Cht_laser) may be related to the higher amount of chitosan particles exposed at the surface and, in addition, to the increment in surface roughness when compared with non-processed samples. It was expected that the material surface would become more hydrophilic, since chitosan is rich in polar groups (–OH and $–NH_2$). Therefore, its presence in the composite resulted in a significant decrease of the water contact angle. The same effect was previously reported (Coutinho *et al.*, 2008) for the PBS/Cht composite when the thin surface layer was removed by plasma etching, but in the cited report the contact angle obtained after processing was 78°.

3.2. Surface chemistry characterization

To further investigate the chemical differences between laser-processed and non-processed PBS/Cht composites, ATR–FTIR analysis was performed and is presented in the spectra of Figure 4. The characteristic absorption bands are assigned to the components of the composite: O–H and N–H (3480–3080 cm^{-1}), CH_2 (2960–2560 cm^{-1}), C═O (1648 cm^{-1}), NH_2 (1396 cm^{-1}), C–O and C–N (1139–915 cm^{-1}) are assigned to chitosan; C═O (1713 cm^{-1}), C–O (1157 cm^{-1}) and C–H (1147–1263 cm^{-1}) are assigned to PBS (Coutinho *et al.*, 2008). The data from the ATR–FTIR showed an increased intensity in the bands of the laser-processed PBS–Cht samples, but no significant differences were observed between irradiated and non-irradiated samples.

Due to the insufficient sensitivity of the FTIR spectroscopy technique to evaluate variations in the chemical composition, a complementary study on the surface chemistry was performed with XPS. Semi-quantitative data from laser-processed and non-processed samples are summarized in Table 1. The spectrum of PBS showed mainly the presence of carbon and oxygen, as expected according to the chemical structure of the components, although N (0.5 %), Si (1.2 %), Ca (0.3 %) and Na (1.3 %) were also detected in trace amounts. The spectrum of chitosan showed the presence of carbon, oxygen and nitrogen as major elements, but also Si (0.7 %), Ca (0.6 %), Na (0.6 %) and Mg (1.2 %) were detected. The nitrogen-containing groups (–NH–and $–NH_2$) are the functional groups allowing discrimination between the composition of PBS and that of chitosan. Only traces of nitrogen are detected for the PBS/Cht samples, according to the skin–core morphology of the discs. However, laser ablation of the external PBS layer from the composite discs induced an increment of chitosan content, as identified by the increased amount of nitrogen (Table 1).

Table 1. Chemical composition of chitosan, PBS, non-processed PBS/Cht and laser-processed PBS/Cht (PBS/Cht_laser), as determined by XPS

Sample	C_{1s} (%)	N_{1s} (%)	O_{1s} (%)	C : O ratio	C : N ratio
Chitosan	60.4	5.7	30.8	1 : 0.51	1 : 0.094
PBS	80.1	0.5	16.7	1 : 0.21	1 : 0.006
PBS/Cht	71.0	0.3	26.9	1 : 0.38	1 : 0004
PBS/Cht_laser	71.6	1.0	26.1	1 : 0.36	1 : 0.014

The C1s core level spectrum of chitosan reveals several different peaks whose positions can be associated with the functional groups of chemical bonds, such as C–C, C–H, C–O and O–C═O. In our analysis, we assumed that the chitosan C1s spectra were represented by three different environments. Figure 5 and Table 2 show that the C1s peak at 285.0 eV belongs to the main backbone carbon bonds (C–H and C–C), which overlap the $C–NH_2$ from the glucosamine rings existing in chitosan (Lopez-Perez *et al.*, 2007; Silva *et al.*, 2008). Because of the binding

DOI: 10.1002/term

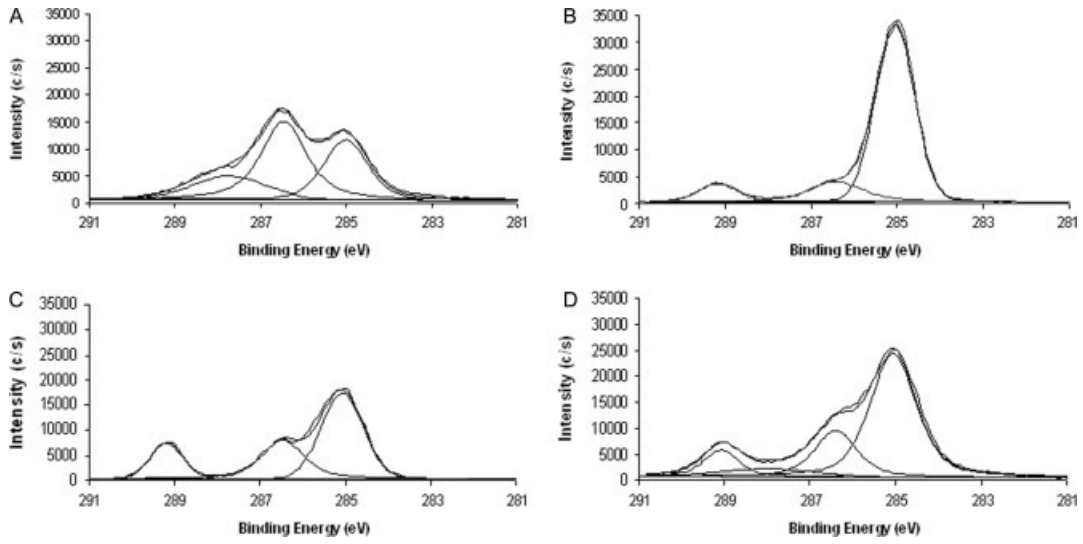

Figure 5. C_{1s} **core level spectra of non-processed chitosan (A), PBS (B), PBS/Cht discs (C) and laser-processed PBS/Cht (D) discs**

Table 2. C_{1s} **core level spectra of chitosan, PBS, non-processed PBS/Cht and laser-processed PBS/Cht (PBS/Cht_laser)**

Sample	Binding energy, eV (relative intensity, %)	Assignments
Chitosan	285.0 (36.8)	C–C, C–H and C–NH_2
	286.4 (47.7)	C–O
	287.7 (15.5)	C═O
PBS	285.0 (81.3)	C–C and C–H
	286.4 (9.9)	C–O
	289.2 (8.8)	O═C–O
PBS/Cht	285.0 (53.1)	C–C, C–H and C–NH_2
	286.4 (24.5)	C–O
	289.2 (22.4)	O═C–O
PBS/Cht_laser	285.2 (58.5)	C–C, C–H and C–NH_2
	286.4 (22.7)	C–O
	287.9 (5.2)	C═O
	289.1 (13.6)	O═C–O

energy overlap, these bonds are considered to be one component. The peak present at 286.4 eV was assigned to C–O, C–OH and C–N–C═O and the peak at 287.7 eV to C═O and N–C═O chemical bonds. As seen in Figure 5b, PBS exhibited three characteristic peaks of C1s. The first peak (285.0 eV) was attributed to the aliphatic carbon bonds or the hydrocarbon backbone (C–C and C–H). The second peak (286.4 eV) was attributed to the C1s of ether bonds (C–O) and the third peak (289.2 eV) was ascribed to the O═C–O bonds (Kim and Kim, 2008). PBS/Cht non-processed discs spectra in Figure 5c and Table 2, being a composite, show the characteristics groups of each polymer. The laser-processed PBS/Cht samples shown in Figure 5d have a new band in the C1s high-resolution spectra (287.9 eV) that is not detected in the non-processed PBS/Cht. This is a characteristic of chitosan, corresponding to the carbonyl bonds (C═O), associated with an increased intensity of the peak at 285.2 eV (NH_2). This result confirmed the exposure of the chitosan phase, promoted by the laser etching upon removal of the thin outer layer of PBS. Those observations corroborate, and are in close agreement with, the results obtained in the ATR–FTIR and water contact angle measurements.

The chemical composition of the surfaces was further analysed by ToF–SIMS. Positive and negative SIMS spectra are shown in Figure 6a, b. The main result is that the spectra corresponding to the non-processed and laser-processed PBS/Cht discs are very similar and only minor differences are observed. In the positive spectrum of PBS, the signal $m/z = 101$ contains a carbonyl (–COOH) group, 147, and 221 includes a hydroxyl (-OH) group, both observed in the laser-processed and non-processed PBS/Cht spectra, with a decrease of peak 147 after laser processing. This confirms the existence of an external PBS-rich layer and a significant content of PBS in the bulk. The major negative peaks of PBS containing oxygen atom(s) are at $m/z = 117$ and 163 and are also detected in both the laser-processed and non-processed PBS/Cht spectra. Comparing the laser-processed and non-processed PBS/Cht samples, both the positive and the negative spectra show the characteristic peaks of chitosan. However, some new peaks are detected that were not observed in the individual components of the composite. The new positive fragments are at $m/z = 142$, 184, 647 and 662 and the negative fragments at $m/z = 205$ and 473. This could indicate the presence of a new chemical entity, caused by either UV chemical modification or any chemical reaction between the two components during injection moulding, which was not previously reported in the literature. Another new fragment was observed in the negative spectrum of laser-processed samples (i.e. $m/z = 457$) containing a carbonyl group (C═O), indicating a modification induced by the laser irradiation apart from the removal of the outer layer of the composite. This fragment ($C_{30}H_{49}O_3$) could be derived from a thermally activated reaction (e.g. by chain scission) caused by the laser ablation of the aliphatic PBS chain (Bityurin, 2005). Overall, the ToF–SIMS analysis is in agreement with the XPS results previously discussed.

DOI: 10.1002/term

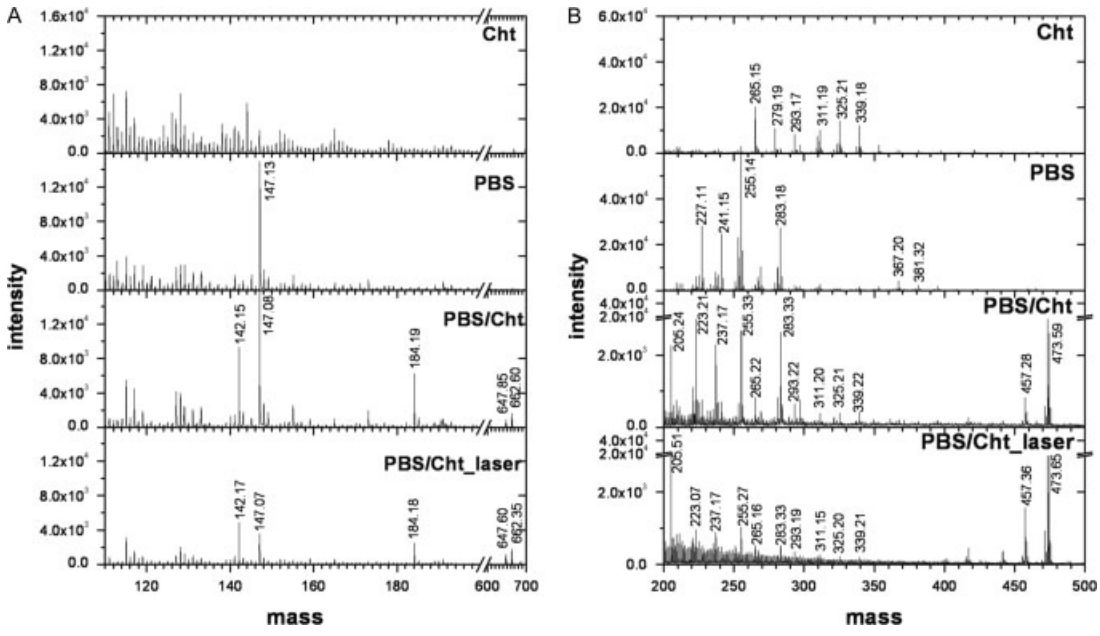

Figure 6. ToF–SIMS spectra of non-processed chitosan, PBS, PBS/Cht and laser-processed PBS/Cht (PBS/Cht_laser) discs: positive (A) and negative (B) modes

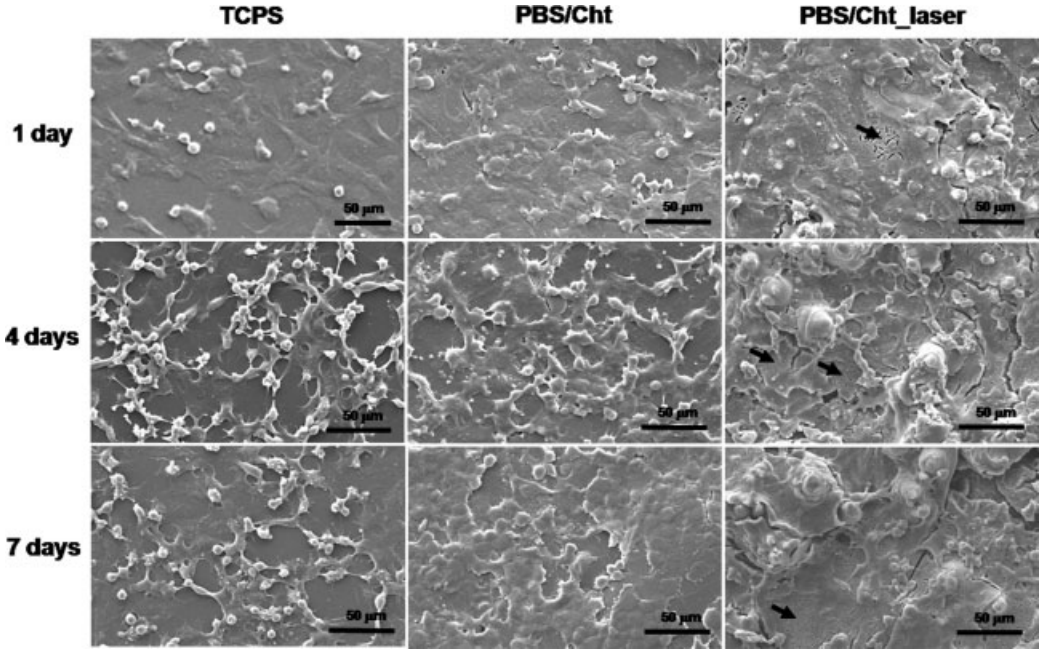

Figure 7. SEM micrographs of human osteoblastic cells (Saos-2 cell line) cultured on TCPS, non-processed PBS/Cht and laser-processed PBS/Cht (PBS/Cht_laser) discs for 1, 4 and 7 days. Arrows indicate the chitosan particles entrapped in the PBS matrix

3.3. Biological performance

A qualitative analysis of the cell morphology and distribution when cultured in standard tissue culture polystyrene (TCPS), laser-processed and non-processed PBS/Cht discs was performed by scanning electron microscopy (SEM). SEM micrographs (Figure 7) show that human osteoblastic cells were able to adhere to the surface of all the tested materials after 1 day of culture. Depending on the surface and/or material, some differences in cell morphology were observed. Cells cultured in TCPS showed the typical polygonal shape and epithelium-like morphology of osteoblastic cells. The non-processed PBS/Cht discs induced higher cell spreading than in the TCPS surface, presenting cytoplasmic extensions and focal adhesion points at the surface. This phenomenon of cellular flattening was even more pronounced in the laser-processed PBS/Cht discs. This surface causes the cells to be more irregular in shape than cells observed in PBS/Cht (non-processed) discs and in TCPS. The analysis of human osteoblast-like cells cultured for longer periods (4 and 7 days) shows

DOI: 10.1002/term

an increase in cell number, presenting evident filopodia over the substrates, particularly in the case of the TCPS control. This observation was not so pronounced in cells cultured on the PBS/Cht discs (non-processed and laser-processed). The surfaces of these samples induce a higher degree of cell spreading, with the absence of cells with round morphology when compared to Saos-2 cells cultured on TCPS. The most important observation in the morphological analysis was the formation of cell multilayer structures on laser-processed PBS/Cht discs. Interestingly, it seems that osteoblasts cultured on this surface tend to prefer PBS-rich areas instead of chitosan-rich areas (arrows in Figure 7). However, there are also differences in topography that do not allow direct conclusions about the chemical nature of this cellular preference.

Considering the qualitative analysis of the cell behaviour, the flat and spread morphology is an indicator of higher metabolic activity than the roundish morphology predominantly observed in TCPS. Despite the morphological alterations observed in human osteoblastic cells cultured on laser-processed surfaces, the cell viability (Figure 8) and proliferation (Figure 9) were not significantly affected. In fact, during the early culture periods, cell viability and proliferation values were comparable for the different materials and/or surfaces.

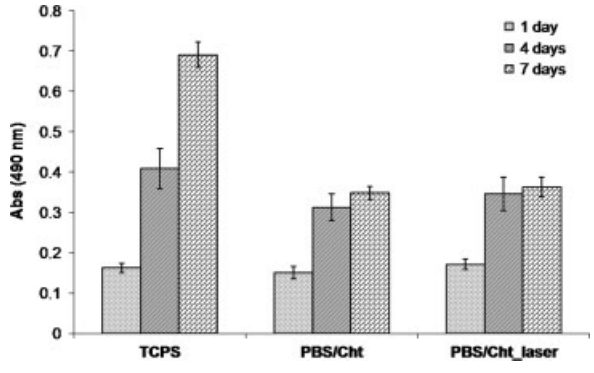

Figure 8. Viability of human Saos-2 cells cultured on TCPS, non-processed PBS/Cht and laser-processed PBS/Cht (PBS/Cht_laser) discs for 1, 4 and 7 days, determined by MTS assay

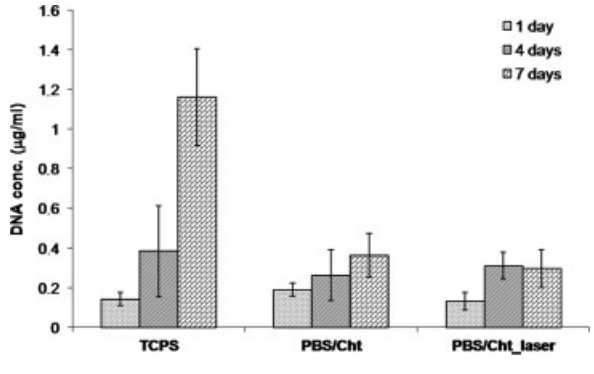

Figure 9. dsDNA quantification of Saos-2 cells cultured on TCPS, non-processed PBS/Cht and laser-processed PBS/Cht (PBS/Cht_laser) discs for 1, 4 and 7 days

This observation demonstrates the reproducibility of the seeding process between samples and also the mild effect of laser processing over the biological performance (i.e. adhesion and metabolic activity). For longer culture periods (7 days), the surfaces of laser-processed and non-processed PBS/Cht discs showed comparable results of cell viability and proliferation. However, those values were much lower for osteoblastic cells cultured on both laser-processed and non-processed PBS/Cht discs than in TCPS.

Modifications of the surface morphology and chemistry can change the surface hydrophilicity, which is one of the key material properties determining the cell–surface material interaction. However, the cell activity seems not to be affected by the observed differences in surface chemistry and, consequently, wettability between the two PBS/Cht samples. The osteoblastic cells tend to prefer adhering to the PBS matrix, avoiding the chitosan-rich areas, and thus their metabolic activity and proliferation are spatially conditioned, which may cause the observed multilayered cellular structures. Indeed, the current biological results do not follow previous reports in the literature showing the importance and the influence of hydrophilicity over cell activity (Groth and Altankov, 1996; Webb *et al*., 1998). Thus, we can only speculate that, considering this cell type and the materials under study, other parameters may be more influential than the wettability of the surface. Another surface property that could help in understanding the biological performance reported here is the surface roughness (Anselme *et al*., 2000a, 2000b). In the present study, no significant differences were found in the biological activity of cells cultured on the smoother surface of non-processed PBS/Cht discs and and those cultured on the rougher surface of laser-processed PBS/Cht discs. In the literature, there is no consensus on the effect or influence of surface roughness on osteoblast adhesion and proliferation: some studies report a negative effect of the surface roughness over cell activity (Anselme *et al*., 2000a, 2000b; Martin *et al*., 1995), whereas other studies show enhanced osteoblastic behaviour (Degasne *et al*., 1999; Hatano *et al*., 1999; Kunzler *et al*., 2007; Lincks *et al*., 1998).

4. Conclusions

PBS/Cht composites were exposed to UV laser ablation for the removal of the external thin PBS layer, and modifications induced by the laser processing evaluated. The amount of chitosan exposed at the surface of laser-processed samples significantly changes the surface morphology and wettability of the samples. Additionally, some chemical differences (appearance of chitosan and other compounds from the treatment) were observed by either XPS or ToF–SIMS between the laser-processed and non-processed samples. Those parameters, however, do not seem to have a significant influence over cell viability and proliferation. The morphology of the cells

DOI: 10.1002/term

was shown to be considerably different in the case of laser-processed samples. Cells aggregate in multilayer columnar structures, preferentially in the PBS matrix, avoiding the chitosan-rich surface.

The biological results obtained in laser-processed surfaces were very similar to those obtained for non-processed samples, suggesting that the laser processing was not detrimental to cell activity. Additionally, the biological performance of the inner regions of the material was not significantly different from those of the outer layer, despite the differences in morphology and wettability. Further studies should be performed in order to understand this cellular response to chitosan particles in a matrix of PBS and to unfold the contributions of surface roughness and chemical composition.

Acknowledgements

This work was partially supported by the European Union Integrated Project GENOSTEM (LSH-STREP-CT-2003-503161), the European Union Network of Excellence EXPERTISSUES (NMP3-CT-2004-500283), the Interreg III Project PROTEUS (SP1P151/03) and Xunta de Galicia (Consolidación 2006/12). The Portuguese Foundation for Science and Technology is also acknowledged for a PhD grant to A.M. (SFRH/BD/24382/2005). The authors wish to thank C. Serra from CACTI of the University of Vigo for the XPS and ToF–SIMS measurements.

References

Agrawal CM, Ray RB. 2001; Biodegradable polymeric scaffolds for musculoskeletal tissue engineering. *J Biomed Mater Res* **55**: 141–150.

Alves CM, Reis RL. 2005; Protein and cell interactions with biodegradable systems. In *Biodegradable Systems in Tissue Engineering and Regenerative Medicine*, Reis RL, San Roman J (eds). CRC Press: Boca Raton, FL.

Anselme K, Bigerelle M, Noel B, *et al*. 2000a; Qualitative and quantitative study of human osteoblast adhesion on materials with various surface roughnesses. *J Biomed Mater Res* **49**: 155–166.

Anselme K, Linez P, Bigerelle M, *et al*. 2000b; The relative influence of the topography and chemistry of TiAl6V4 surfaces on osteoblastic cell behaviour. *Biomaterials* **21**: 1567–1577.

Arpornmaeklong P, Suwatwirote N, Pripatnanont P, *et al*. 2007; Growth and differentiation of mouse osteoblasts on chitosan–collagen sponges. *Int J Oral Maxillofac Surg* **36**: 328–337.

Bityurin N. 2005; Studies on laser ablation of polymers. *Annu Rep Prog Chem C* **101**: 216–247.

Chen J, Li Q, Xu J, *et al*. 2005; Study on biocompatibility of complexes of collagen–chitosan–sodium hyaluronate and cornea. *Artif Organs* **29**: 104–113.

Chuang WY, Young TH, Yao CH, *et al*. 1999; Properties of the poly(vinyl alcohol)/chitosan blend and its effect on the culture of fibroblast *in vitro*. *Biomaterials* **20**: 1479–1487.

Correlo VM, Boesel LF, Bhattacharya M, *et al*. 2005; Properties of melt processed chitosan and aliphatic polyester blends. *Mater Sci Eng A* **403**: 57–68.

Correlo VM, Boesel LF, Pinho E, *et al*. 2009; Melt-based compression-molded scaffolds from chitosan–polyester blends and composites: morphology and mechanical properties. *J Biomed Mater Res* **91A**: 489–504.

Correlo VM, Pinho ED, Pashkuleva I, *et al*. 2007; Water absorption and degradation characteristics of chitosan-based polyesters and hydroxyapatite composites. *Macromol Biosci* **7**: 354–363.

Costa-Pinto AR, Salgado AJ, Correlo VM, *et al*. 2008; Adhesion, proliferation, and osteogenic differentiation of a mouse mesenchymal stem cell line (BMC9) seeded on novel melt-based chitosan/polyester 3D porous scaffolds. *Tissue Eng A* **14**: 1049–1057.

Coutinho DF, Pashkuleva IH, Alves CM, *et al*. 2008; The effect of chitosan on the *in vitro* biological performance of chitosan–poly(butylene succinate) blends. *Biomacromolecules* **9**: 1139–1145.

Cruz DM, Ivirico JL, Gomes MM, *et al*. 2008; Chitosan microparticles as injectable scaffolds for tissue engineering. *J Tissue Eng Regen Med* **2**: 378–380.

Degasne I, Basle MF, Demais V, *et al*. 1999; Effects of roughness, fibronectin and vitronectin on attachment, spreading, and proliferation of human osteoblast-like cells (Saos-2) on titanium surfaces. *Calcif Tissue Int* **64**: 499–507.

Gan Z, Abe H, Kurokawa H, *et al*. 2001; Solid-state microstructures, thermal properties, and crystallization of biodegradable poly(butylene succinate) (PBS) and its copolyesters. *Biomacromolecules* **2**: 605–613.

Gobin AS, Froude VE, Mathur AB. 2005; Structural and mechanical characteristics of silk fibroin and chitosan blend scaffolds for tissue regeneration. *J Biomed Mater Res A* **74**: 465–473.

Gomes ME, Reis RL. 2004; Biodegradable polymers and composites in biomedical applications: from catgut to tissue engineering. Part 1. Available systems and their properties. *Int Mater Rev* **49**: 261–273.

Groth T, Altankov G. 1996; Studies on cell–biomaterial interaction: role of tyrosine phosphorylation during fibroblast spreading on surfaces varying in wettability. *Biomaterials* **17**: 1227–1234.

Hatano K, Inoue H, Kojo T, *et al*. 1999; Effect of surface roughness on proliferation and alkaline phosphatase expression of rat calvarial cells cultured on polystyrene. *Bone* **25**: 439–445.

Honma T, Zhao L, Asakawa N, *et al*. 2006; Poly(ε-caprolactone)/chitin and poly(ε-caprolactone)/chitosan blend films with compositional gradients: fabrication and their biodegradability. *Macromol Biosci* **6**: 241–249.

Hutmacher DW, Schantz JT, Lam CX, *et al*. 2007; State of the art and future directions of scaffold-based bone engineering from a biomaterials perspective. *J Tissue Eng Regen Med* **1**: 245–260.

Im SY, Cho SH, Hwang JH, *et al*. 2003; Growth factor releasing porous poly(ε-caprolactone)–chitosan matrices for enhanced bone regenerative therapy. *Arch Pharm Res* **26**: 76–82.

Kim HS, Kim HJ. 2008; Enhanced hydrolysis resistance of biodegradable polymers and biocomposites. *Polym Degrad Stabil* **93**: 1544–1553.

Kim IY, Seo SJ, Moon HS, *et al*. 2007; Chitosan and its derivatives for tissue engineering applications. *Biotechnol Adv* **26**: 1–21.

Kolhe P, Kannan RM. 2003; Improvement in ductility of chitosan through blending and copolymerization with PEG: FTIR investigation of molecular interactions. *Biomacromolecules* **4**: 173–180.

Koyano T, Minoura N, Nagura M, *et al*. 1998; Attachment and growth of cultured fibroblast cells on PVA/chitosan-blended hydrogels. *J Biomed Mater Res* **39**: 486–490.

Kunzler TP, Drobek T, Schuler M, *et al*. 2007; Systematic study of osteoblast and fibroblast response to roughness by means of surface-morphology gradients. *Biomaterials* **28**: 2175–2182.

Lincks J, Boyan BD, Blanchard CR, *et al*. 1998; Response of MG63 osteoblast-like cells to titanium and titanium alloy is dependent on surface roughness and composition. *Biomaterials* **19**: 2219–2232.

Liu H, Yin Y, Yao K. 2007; Construction of chitosan–gelatin–hyaluronic acid artificial skin *in vitro*. *J Biomater Appl* **21**: 413–430.

Lopez-Perez PM, Marques AP, da Silva RMP, *et al*. 2007; Effect of chitosan membrane surface modification via plasma induced polymerization on the adhesion of osteoblast-like cells. *J Mater Chem* **17**: 4064–4071.

Lutolf MP, Hubbell JA. 2005; Synthetic biomaterials as instructive extracellular microenvironments for morphogenesis in tissue engineering. *Nat Biotechnol* **23**: 47–55.

Ma L, Gao C, Mao Z, *et al*. 2003; Collagen/chitosan porous scaffolds with improved biostability for skin tissue engineering. *Biomaterials* **24**: 4833–4841.

Majima T, Irie T, Sawaguchi N, *et al*. 2007; Chitosan-based hyaluronan hybrid polymer fibre scaffold for ligament and tendon tissue engineering. *Proc Inst Mech Eng H* **221**: 537–546.

Malafaya PB, Gomes ME, Salgado AJ, *et al*. 2003; Polymer based scaffolds and carriers for bioactive agents from different natural origin materials. *Adv Exp Med Biol* **534**: 201–233.

Mano JF, Silva GA, Azevedo HS, *et al*. 2007; Natural origin biodegradable systems in tissue engineering and regenerative medicine: present status and some moving trends. *J R Soc Interface* **4**: 999–1030.

Martin JY, Schwartz Z, Hummert TW, *et al*. 1995; Effect of titanium surface roughness on proliferation, differentiation, and protein synthesis of human osteoblast-like cells (MG63). *J Biomed Mater Res* **29**: 389–401.

Mucha M, Pawlak A. 2005; Thermal analysis of chitosan and its blends. *Thermochim Acta* **427**: 69–76.

Oliveira JT, Correlo VM, Sol PC, *et al*. 2008; Assessment of the suitability of chitosan/polybutylene succinate scaffolds seeded with mouse mesenchymal progenitor cells for a cartilage tissue engineering approach. *Tissue Eng* **14**: 1651–1661.

Pinho ED, Martins A, Araújo JV, *et al*. 2009; Degradable particulate composite reinforced with nanofibres for biomedical applications. *Acta Biomater* **5**: 1104–1114.

Ray SS, Okamoto K, Maiti P, *et al*. 2002; New poly(butylene succinate)/layered silicate nanocomposites: preparation and mechanical properties. *J Nanosci Nanotechnol* **2**: 171–176.

Rinaudo M, Milas M, Le Dung P. 1993; Characterization of chitosan. Influence of ionic strength and degree of acetylation on chain expansion. *Int J Biol Macromol* **15**: 281–285.

Salgado AJ, Coutinho OP, Reis RL. 2004; Bone tissue engineering: state of the art and future trends. *Macromol Biosci* **4**: 743–765.

Sarasam A, Madihally SV. 2005; Characterization of chitosan–polycaprolactone blends for tissue engineering applications. *Biomaterials* **26**: 5500–5508.

Silva SS, Luna SM, Gomes ME, *et al*. 2008; Plasma surface modification of chitosan membranes: characterization and preliminary cell response studies. *Macromol Biosci* **8**: 568–576.

Subramanian A, Vu D, Larsen GF, *et al*. 2005; Preparation and evaluation of the electrospun chitosan/PEO fibers for potential applications in cartilage tissue engineering. *J Biomater Sci Polym Ed* **16**: 861–873.

Vandevord PJ, Matthew HW, Desilva SP, *et al*. 2002; Evaluation of the biocompatibility of a chitosan scaffold in mice. *J Biomed Mater Res* **59**: 585–590.

Wan Y, Wu H, Yu A, *et al*. 2006; Biodegradable polylactide/chitosan blend membranes. *Biomacromolecules* **7**: 1362–1372.

Webb K, Hlady V, Tresco PA. 1998; Relative importance of surface wettability and charged functional groups on NIH 3T3 fibroblast attachment, spreading, and cytoskeletal organization. *J Biomed Mater Res* **41**: 422–430.

Wu X, Black L, Santacana-Laffitte G Jr, *et al*. 2007; Preparation and assessment of glutaraldehyde-crosslinked collagen–chitosan hydrogels for adipose tissue engineering. *J Biomed Mater Res A* **81**: 59–65.

Zivanovic S, Li J, Davidson PM, *et al*. 2007; Physical, mechanical, and antibacterial properties of chitosan/PEO blend films. *Biomacromolecules* **8**: 1505–1510.

DOI: 10.1002/term